

DMD #32326

Metabolism of Flumatinib, a Novel Antineoplastic Tyrosine Kinase Inhibitor, in Chronic Myelogenous Leukemia Patients

Aishen Gong, Xiaoyan Chen, Pan Deng and Dafang Zhong

Shanghai Institute of Materia Medica, Chinese Academy of Sciences, Shanghai, China (A.G., X. C., P. D.,
D. Z.)

Shanghai Hengrui Pharmaceutical Co., Ltd., Shanghai, China (A.G.)

DMD #32326

Running Title

Metabolism of Flumatinib in CML Patients

Corresponding Author: Dafang Zhong

Shanghai Institute of Materia Medica, Chinese Academy of Sciences, 646 Songtao Road, Shanghai 201203,

China

Phone: 0086-21-50800738

Fax: 0086-21-50800738

Email: dfzhong@mail.shenc.ac.cn

Number of text pages: 22 (Without Refs)

Number of tables: 2

Number of figures: 9

Number of references: 12

Number of words in the Abstract: 215

Number of words in the Introduction: 217

Number of words in the Discussion: 928

Abbreviations: CML, chronic myelogenous leukemia; UPLC, ultra-performance liquid chromatography;

Q-TOF MS, quadrupole time-of-flight mass spectrometer; MDF, mass defect filtering.

DMD #32326

Abstract

Flumatinib (HH-GV678, 4-(4-methyl-piperazin-1-ylmethyl)-*N*-[6-methyl-5-(4-pyridin-3-yl-pyrimidin-2-ylamino)-pyridin-3-yl]-3-trifluoromethyl-benzamide), an antineoplastic tyrosine kinase inhibitor, is currently in phase I clinical trials in China for the treatment of chronic myelogenous leukemia (CML). The purpose of this study was to identify the metabolites of flumatinib in CML patients, with the aim of determining the main metabolic pathways of flumatinib in humans after oral administration. Ultra performance liquid chromatography/Q-TOF mass spectrometry revealed 34 metabolites; 7 primary metabolites were confirmed by comparison with synthetic reference standards. The results show that the parent drug flumatinib was the main form recovered in human plasma, urine and feces. The main metabolites of flumatinib in human were the products of *N*-demethylation, *N*-oxidation, hydroxylation and amide hydrolysis. In addition to these phase I metabolites, several phase II glucuronidation and acetylation products were detected in plasma, urine and feces. The observed circulating metabolites included an *N*-demethylated metabolite (M1), two hydrolytic metabolites (M3, M4), oxidation metabolites (M2-1, M2-4, M2-7, M2-9 and M14), a glucuronide conjugate (M16-2) and several multiple metabolic products. Flumatinib was predominantly metabolized by amide bond cleavage to yield two corresponding hydrolytic products. By comparison with the related drug imatinib (4-(4-methyl-piperazin-1-ylmethyl)-*N*-[4-methyl-3-(4-pyridin-3-yl-pyrimidin-2-ylamino)-phenyl]-benzamide), we concluded that the electron-withdrawing groups of trifluoromethyl and pyridine facilitated the amide bond cleavage and led to the *in vivo* formation of a carboxylic acid and an amine.

Introduction

Chronic myelogenous leukemia (CML) is a chronic myeloproliferative disease that is characterized by an overproduction of immature myeloid cells and mature granulocytes. A reciprocal chromosome translocation $t(9; 22)$, called the Philadelphia chromosome, causes a constitutive activation of the BCR-ABL tyrosine kinase and leads to the development of CML (Ren 2005; Deininger et al., 2000). For this reason, current CML treatment strategies involve the use of tyrosine kinase inhibitors such as imatinib, nilotinib and dasatinib (Sawyers et al., 2001; Steinberg et al., 2007; Kantarjian et al., 2006). Flumatinib, a structural analogue of imatinib, is currently undergoing phase I clinical trials in China, in oral form as its mesylate salt. Previous nonclinical studies have shown flumatinib to have more potent *in vitro* and *in vivo* activity than imatinib when tested against leukemia cells expressing BCR-ABL (Sun et al., 2008). The current clinical trials are being performed to assess tolerability and pharmacokinetic properties of flumatinib, as well as to determine its initial therapeutic efficacy in CML patients.

The objective of the present study was to investigate the metabolism of flumatinib in CML patients using an ultra-performance liquid chromatography-quadrupole time-of-flight mass spectrometry (UPLC/Q-TOF MS) method. The metabolic profiles of flumatinib in plasma, urine and feces were characterized following its oral administration to CML patients enrolled in the clinical study.

DMD #32326

Materials and methods

Chemicals. Flumatinib mesylate tablets were manufactured by Jiangsu Hansoh Pharmaceutical Co., Ltd. (Lianyungang, China) and used for phase I clinical trials. Reference substances for flumatinib mesylate, *N*-desmethyl metabolite (M1), M3, M4, M5, M20 and imatinib mesylate were also kindly provided by Hansoh Pharm. The *N*-oxide of flumatinib (M2-9) and *N*-acetylated M4 (M10) were synthesized and purified in our laboratory. Gradient grade acetonitrile and HPLC grade formic acid were purchased from Sigma-Aldrich (St. Louis, MO, USA). Purified water was generated by a Millipore Milli-Q Gradient Water Purification System (Molsheim, France).

Subjects and sample collection. The study protocol was previously approved by the Ethics Committee of the Institute of Hematology and Blood Diseases Hospital, Chinese Academy of Medical Sciences & Peking Union Medical College. CML patients in accelerated phase or in the blast crisis phase, 18-65 years old, were enrolled in the tolerability and pharmacokinetic study. Plasma, urine and feces samples before and after oral administration of flumatinib mesylate had been collected for the pharmacokinetic study. We used the remaining samples from this previous trial for the present metabolism studies. All samples had been stored at -20°C until analysis.

Preparation of plasma, urine, and feces samples for metabolite analysis. Human plasma samples had been collected 3 h, 8 h and 12 h postdose. Urine samples had been collected over a 0 to 12 h collection interval after administration. These collected samples were pooled to form a single plasma sample and a single urine sample. A 500 µl aliquot of pooled sample was diluted with water of the same volume, and the mixture was vortexed and centrifuged at 5,000 *g* for 5 min (4°C). The supernatant was passed through an Oasis[®] HLB SPE cartridge (1CC, 30 mg; Waters Corp., Milford, MA, USA) preconditioned with 1 ml methanol and 2 ml water. The cartridge was washed with 1 ml water and eluted with 2 ml methanol. The

DMD #32326

eluate was evaporated to dryness under a stream of nitrogen gas at 40°C in a Turbo Vap evaporator (Zymark Corp., Hopkinton, MA, USA). The residue was reconstituted in 150 µl water: acetonitrile: formic acid (90: 10: 0.05, v/v) and centrifuged at 16,000 g for 5 min (4°C). A 10 µl aliquot of the supernatant was injected into the UPLC/Q-TOF MS system.

A 20 mg feces sample was mixed with 2 ml methanol and homogenized, then extracted by ultrasonication. After centrifugation at 16,000 g for 15 min (4°C), the supernatant was evaporated to dryness under a stream of nitrogen gas at 40°C. The residue was reconstituted in 300 µl of water: acetonitrile: formic acid (90: 10: 0.05, v/v) and centrifuged at 16,000 g for 5 min (4°C). A 2 µl aliquot of the supernatant was injected into the UPLC/Q-TOF MS system.

To identify the *N*-oxides, the biological matrices were treated with a reductant titanium trichloride (TiCl₃), which can selectively reduce *N*-oxides to their corresponding amines (Seaton et al., 1984; Kulanthaivel et al., 2004). TiCl₃ (5 µl) was added to a 500 µl aliquot of urine or a 2 ml aliquot of feces extraction. After 90 min at 0 °C, they were treated as described before and analyzed.

UPLC and mass spectrometer apparatus. Chromatographic separation was performed using a Waters Acquity UPLC[®] system (Waters Corp., Milford, MA, USA), equipped with a binary solvent delivery system, column oven and autosampler. Mass spectrometry was performed on a Synapt[™] quadrupole time-of-flight mass spectrometer (Q-TOF; Waters Corp., Milford, MA, USA) equipped with an electrospray ionization source (ESI). The raw data were acquired and processed by the Masslynx[™] Version 4.1, MetaboLynx[™] and MassFragment[™] software (Waters Corp., Milford, MA, USA). A LCQ Advantage[™] ion trap spectrometer (ThermoFinnigan Corp., San Jose, CA, USA) equipped with an electrospray ionization source (ESI) was used for the fragmentation study.

UPLC conditions. Chromatographic separations were achieved on an Acquity UPLC BEH column

DMD #32326

(2.1×100 mm, 1.7 μm; Waters Corp., Milford, MA, USA) thermostated at 40°C. The autosampler was maintained at 10°C. The components were eluted with a gradient of formic acid (0.05%) in water (mobile phase A) versus formic acid (0.05%) in acetonitrile (mobile phase B) at a flow rate of 0.5 ml/min. The gradient elution program was: 98% A at 0 min, 98 to 95% A at 0 to 4 min, 95 to 80% A at 4 to 22 min, 80 to 20% A at 22 to 24 min, 20 to 0% A at 24 to 26 min and 0 to 98% A at 26 to 30 min. The system was equilibrated at 98% A for 4 min before the next run.

Q-TOF MS conditions. Mass spectrometry was performed in the positive ion mode electrospray. The capillary and cone voltages were 1500 and 50 V, respectively. The desolvation gas (nitrogen) was set to 800 l/h at a temperature of 400°C and the source temperature was 120°C. Data were acquired from 50 to 1000 Da and corrected during acquisition using an external reference (Lock SprayTM) comprised of a solution of 600 ng/ml leucine encephalin (m/z 556.2771) infused at 5 μl/min. A MS^E scan function was programmed with two independent collision energies (CE). At low collision energy, the transfer CE and trap CE were 4 eV and 6 eV, respectively. At high collision energy, the transfer CE and trap CE were 4 eV and were ramped from 25 to 35 eV, respectively. In this manner, precursor ion and fragmentation information were obtained in one sample run (Bateman et al., 2007).

LCQ ion trap MS conditions. To elucidate the MS fragmentation pathways, MSⁿ mass spectra were obtained in the ESI positive ion mode. Nitrogen was used as the sheath gas (35 arb). No auxiliary gas was used. The spray and capillary voltages were set at 4.5 kV and 30 V, respectively. The capillary temperature was set to 200 °C. Samples were introduced into the mass spectrometer by syringe pump. MSⁿ mass spectra were obtained by collision-induced dissociation (CID). The collision energy was adjusted to provide characteristic fragment ions of each precursor ion.

Flumatinib metabolite profiling in patient plasma, urine and feces. For the metabolite identification of

DMD #32326

flumatinib, plasma, urine and feces extracts were injected into the UPLC/Q-TOF MS system. Data acquisition and processing were performed using MS^E with the mass defect filtering (MDF) approach (Bateman et al., 2007; Zhang et al., 2008). For each metabolite chromatographic peak found, its corresponding precursor and fragment ions were available from the mass spectra obtained at low and high collision energy, respectively. The elemental composition of each metabolite and its structure were analyzed by MetaboLynxTM software.

Results

Mass spectral fragmentation study of flumatinib. Flumatinib (100 ng/ml) was injected and analyzed using UPLC/MS^E Q-TOF MS to obtain its mass spectral information at low and high collision energy. The mass spectrum of flumatinib at high collision energy is shown in Fig. 2. Flumatinib eluted at 19.2 min. The parent drug produced m/z 563.249 ($M+H^+$) and m/z 585.238 ($M+Na^+$) precursor ions. The main fragment ions of m/z 563.249 were observed at m/z 503.232, 463.148 (100% abundance), 449.136 and 263.105. The elemental composition of these fragment ions was elucidated by the measured accurate mass. The major fragment ion at m/z 463.148 was formed by the neutral loss of the *N*-methylpiperazine moiety. Further neutral loss of one to three HF moieties from m/z 563.249 and 463.148 produced fragment ions at m/z 543.239, 523.239, 503.232 and 423.136. Amide bond cleavage produced fragment ions at m/z 277.121 and 285.124. A minor fragment ion at m/z 545.239 was proposed to be the result of the loss of H₂O. The mass spectra of imatinib at low and high collision energy were obtained as the same way. The precursor ions were observed at m/z 494.265 ($M+H^+$) and m/z 516.249 ($M+Na^+$). The major fragment ion at m/z 394.166 was formed by the neutral loss of the *N*-methylpiperazine moiety, which was the same as that of flumatinib. The proposed mass spectral fragmentation patterns of flumatinib and imatinib are shown in Fig. 2.

The expected metabolite chromatograms for plasma, urine and feces are shown in Fig. 3.

Metabolite characterization. Table 1 lists the possible metabolites of flumatinib including the retention time of each chromatographic peak, proposed elemental composition, and the characteristic mass spectral fragmentation ions. The metabolite structures were characterized by mass spectral fragmentation patterns and, where possible, confirmed by comparison of chromatographic retention times and mass spectra with the chemically synthesized reference standards.

Parent drug M0. A chromatographic peak at 19.2 min was detected in human plasma, urine and feces. Its

DMD #32326

elemental composition was $C_{29}H_{29}F_3N_8O$ and its protonated molecular weight was 563.248. The retention time and mass spectral fragmentation patterns were identical to the parent drug flumatinib, indicating that this component was unmetabolized flumatinib. It was designated as M0 and was the most abundant component in plasma and feces. The standard compound was characterized as: 1H NMR (400 MHz, DMSO) δ : 10.64 (s, 1 H), 9.30 (dd, $J=2.4, 0.8$ Hz, 1 H), 9.18 (s, 1 H), 8.69 (dd, $J=4.8, 1.6$ Hz, 1 H), 8.63 (d, $J=2.0$ Hz, 1 H), 8.57 (dd, $J=4.0, 1.2$ Hz, 2 H), 8.51 (m, 1 H), 8.33 (s, 1 H), 8.29 (m, 1 H), 7.95 (d, $J=8.4$ Hz, 1 H), 7.54 (m, 1 H), 7.51 (d, $J=5.2$ Hz, 1 H), 3.81 (s, 2 H), 3.41 (brs, 4 H), 3.09 (brs, 2 H), 2.92 (brs, 2 H), 2.83 (s, 3 H), 2.36 (s, 3 H). ^{13}C NMR (400 MHz, DMSO) δ : 164.6, 162.2, 161.3, 160.0, 151.9, 148.7, 148.0, 140.7, 137.2, 135.0, 134.2, 134.1, 134.0, 132.5, 132.2, 131.3, 127.9 (q, $J=30$ Hz), 125.7 (q, $J=5$ Hz), 124.5 (q, $J=273$ Hz), 124.2, 124.0, 108.8, 57.0, 53.2 ($2\times C$), 49.9 ($2\times C$), 42.6, 21.2. The NMR data of flumatinib are shown in Supplemental Data Fig. S1-S4.

Metabolite M1. Metabolite M1, found in plasma, urine and feces, eluted at 19.1 min with protonated molecular weight of 549.234. Its elemental composition was $C_{28}H_{27}F_3N_8O$. M1 was a demethylated form of the parent drug. The major fragment ions at m/z 463.149, 449.134, 263.105 and 262.102 were the same as those of parent drug. Only m/z 100 was lacking, which indicated that the demethylation occurred on the methyl piperazine moiety. The chromatographic retention time and mass spectral fragmentation patterns of M1 were identical to the synthesized reference standard of *N*-desmethyl flumatinib, M1 was accordingly confirmed as the *N*-desmethyl flumatinib, which has been shown to have similar pharmacological properties to the parent drug.

Metabolite M2. Metabolite M2 had a protonated molecular weight of 579.244, which was 16 Da higher than the protonated parent drug. Its elemental composition was $C_{29}H_{29}F_3N_8O_2$, indicating that an oxygen atom had been introduced into the molecule to form an *N*-oxidation or hydroxylation metabolite of M0. Up

DMD #32326

to 4, 7, and 9 chromatographic peaks with a protonated ion at m/z 579.244 were detected in extracts of plasma, urine and feces, respectively. These oxides were numbered according to their order of chromatographic retention time and the structures were elucidated by their mass spectral fragments. The chromatograms of human urine and feces reduced and unreduced by $TiCl_3$ are shown in Supplemental Data Fig. S13-S14.

Metabolites M2-1 and M2-6 eluted at 16.2 min and 18.5 min, respectively. The major fragment ion at m/z 479.146 showed the oxygen was introduced into part B (Fig. 4). Treatment with $TiCl_3$ resulted in the disappearance of these two peaks, which suggested that M2-1 and M2-6 were *N*-oxides. We therefore proposed that an oxygen atom was introduced into part A to form *N*-oxidation metabolites. The fragment ion at m/z 463.148 was formed by the loss of the oxygen atom (-16 Da) from part B. While the m/z 263.105 and 262.104 fragment ions were produced accordingly. The oxidation position was not clear.

Metabolites M2-2, M2-3, M2-4, M2-5 and M2-7 eluted at 16.4, 17.0, 17.6, 18.4 and 19.6 min, respectively. The same major fragment ions at m/z 479.147 and 279.093 were 16 Da larger than the fragment ions at m/z 463.148 and 263.105 of the parent drug, respectively; indicating that part A (Fig. 4) was oxidized. Other fragment ions at m/z 278.101 of M2-4 and M2-7 were 16 Da higher than m/z 262.102 of the parent drug, showing that the amido nitrogen was intact. Treatment with $TiCl_3$ resulted in the reduced peak area of M2-7, which suggested that M2-7 was an *N*-oxide.

Metabolite M2-8 eluted at 20.2 min. The high abundance fragment ion at m/z 561.234 resulted from a neutral loss of H_2O which indicated the formation of a hydroxyl group on the parent drug moiety. Since the other major fragment ion at m/z 462.140 showed that part B was intact, we tentatively identified M2-8 as a metabolite hydroxylated at the methyl piperazine group. M2-8 eluted after M0 due to the formation of an intramolecular hydrogen bond between the hydroxyl hydrogen and hydrogen acceptor nitrogen which led to

DMD #32326

the lower polarity of the moiety.

Metabolite M2-9, found in all three samples, eluted at 21.3 min. The primary fragment ion was m/z 464.160, which resulted from the formation of a radical ion by the loss of the methyl piperazine moiety, suggesting that part B was intact and that the oxygen atom was introduced into the methyl piperazine group. The mass spectral fragmentation patterns were similar to unchanged flumatinib except for the appearance of fragment ions at m/z 492.178 and 116.052, which confirmed the oxidation of the methyl piperazine group. Treatment with $TiCl_3$ resulted in the disappearance of the peak corresponding to M2-9, which suggested that M2-9 was an *N*-oxide. The standard reference was synthesized chemically using *m*-chloroperoxybenzoic acid (MCPBA) and the reaction temperature was kept at $-20^\circ C$. The NMR spectra data (including 1H and ^{13}C) confirmed the proposed structure and provided the positional information of the oxygen atom. The standard compound was characterized as: 1H NMR (400 MHz, DMSO) δ : 10.91 (s, 1 H), 9.30 (s, 2 H), 8.69 (dd, $J=4.4, 1.2$ Hz, 1 H), 8.64 (d, $J=2.0$ Hz, 1 H), 8.56 (m, 2 H), 8.50 (m, 1 H), 8.30 (s, 1 H), 8.27 (d, $J=8.4$ Hz, 1 H), 7.92 (d, $J=8.4$ Hz, 1 H), 7.53 (m, 1 H), 7.51 (d, $J=5.2$ Hz, 1 H), 3.76 (s, 2 H), 3.39 (m, 2 H), 3.08 (s, 3 H), 2.89 (m, 4 H), 2.54 (s, 2 H), 2.46 (s, 3 H). ^{13}C NMR (400 MHz, DMSO) δ : 164.8, 162.2, 161.3, 160.0, 152.0, 148.7, 148.1, 141.3, 137.4, 135.0, 134.2, 134.1, 134.0, 132.5, 132.2, 131.3, 127.8 (q, $J=30$ Hz), 125.7 (q, $J=6$ Hz), 124.6 (q, $J=272$ Hz), 124.3, 124.0, 108.7, 65.4 ($2\times C$), 60.2, 57.2, 47.6 ($2\times C$), 21.3. The NMR data of M2-9 are shown in Supplemental Data Fig. S5-S8. The mass spectra of M2 and proposed mass fragmentation patterns are shown in Fig. 4.

Metabolite M3. Metabolite M3, found in plasma and urine, eluted at 11.0 min and had a protonated molecular weight of 303.132, with an elemental composition of $C_{14}H_{17}F_3N_2O_2$. This metabolite was the most abundant metabolite in plasma and urine. A fragment ion at m/z 203.032 resulted from a neutral loss of the methyl piperazine moiety, which was similar to that of the parent drug. The primary fragment ion of

DMD #32326

protonated M3 was at m/z 175.037, its elemental composition was proposed to be $C_8H_6F_3O$. To elucidate the mass fragmentation pathways, an MS^n scan was performed on a LCQ AdvantageTM ion trap spectrometer. Fig. 5 shows the MS to MS^5 mass spectra and the proposed mass spectral fragmentation routes of M3. By comparing the chromatographic retention time and mass spectrum with that of the synthesized reference standard, metabolite M3 was confirmed as the amide hydrolytic product of flumatinib which formed a carboxylic acid.

Metabolite M4. Metabolite M4, found in plasma and urine, eluted at 5.8 min and had a protonated molecular weight of 279.136, with an elemental composition of $C_{15}H_{14}N_6$. The major mass spectral fragment ion at m/z 262.111 resulted from the neutral loss of the NH_3 moiety. Other major fragment ions at m/z 78.035, 156.058, 173.084, 235.099 were produced from C-C, C-N bond cleavage or the cleavage across pyridine ring (See Fig. 6). By comparing its chromatographic retention time and mass spectrum with that of the synthesized reference standard, M4 was confirmed as the amide hydrolytic product of flumatinib which formed an amine. The standard compound was characterized as: 1H NMR (400 MHz, DMSO) δ : 9.23 (s, 1H), 8.68 (d, $J = 4.4$ Hz, 1H), 8.49 (d, $J = 5.2$ Hz, 1H), 8.40 (d, $J = 8.0$ Hz, 1H), 7.66 (d, $J = 2.0$ Hz, 1H), 7.53 (dd, $J = 8.0, 4.8$ Hz, 1H), 7.40 (d, $J = 5.2$ Hz, 1H), 7.22 (dd, $J = 6.0, 2.2$ Hz, 1H), 2.26 (s, 3H). ^{13}C NMR (400 MHz, DMSO) δ : 162.1, 161.4, 159.9, 151.8, 148.8, 143.4, 140.0, 134.8, 134.1, 132.6, 132.0, 124.3, 117.6, 108.2, 20.3. The NMR data of M4 are shown in Supplemental Data Fig. S9-S10.

Metabolite M5. Metabolite M5, found in plasma and urine, eluted at 10.5 min and had a protonated molecular weight of 289.112 and a molecular formula of $C_{13}H_{15}F_3N_2O_2$, indicating a demethylation ($-CH_2$) of M3. The major mass spectral fragment ions at m/z 203.033 and 175.037 were similar to those of M3 except for the disappearance of m/z 100, suggesting a modification on the methyl piperazine group. The minor fragment ion at m/z 85.078 further proved that M5 was the *N*-demethylation product of M3. Hence,

DMD #32326

M5 was proposed as the piperazine *N*-desmethyl metabolite of M3 and its structure was confirmed by comparison with the synthesized reference standard.

Metabolite M6. Metabolite M6, found in plasma and urine, eluted at 15.2 min and gave a precursor ion at m/z 319.126 with a mass 16 Da larger than M3 and an elemental composition of $C_{14}H_{17}F_3N_2O_3$, indicating that M6 was an monoxide of M3 (m/z 303.132, $C_{14}H_{17}F_3N_2O_2$). The low abundance fragment ion at m/z 301.115 resulted from a neutral loss of H_2O . The mass spectrum of M6 showed two major fragment ions at m/z 203.030 and 175.039, indicating that oxidation occurred on the methyl piperazine moiety. By comparing the retention times of M3 (11.0 min) and M6 (15.2 min), M6 showed lower polarity than M3, suggesting M6 was probably an *N*-oxide of M3. Treatment of urine sample with $TiCl_3$ resulted in the disappearance of the peak corresponding to M6. The chromatograms of human urine reduced and unreduced by $TiCl_3$ are shown in Supplemental Data Fig. S15. These data further suggested that M6 was an *N*-oxide. A fragment ion at m/z 258.076 indicated the oxidation site to be the nitrogen atom connected with the methyl group (See Fig. 7).

Metabolite M7. Metabolite M7 eluted at 7.6 min in urine and gave a protonated ion at m/z 317.113 with a larger mass of 14 Da than M3 and its elemental composition was $C_{14}H_{15}F_3N_2O_3$, indicating the introduction of an oxygen atom with dehydrogenation. Mass spectral fragment ions of M7 were similar to those of M6, and m/z 203.037 and 175.035 suggested that the modification occurred on the methyl piperazine moiety. A fragment ion at m/z 246.070 further indicated the methyl piperazine group underwent oxidation but the position could not be confirmed. Metabolite M7 was tentatively identified as the oxidation product of M3 with carboxide formation (See Fig. 7).

Metabolite M8 and M9. Metabolites M8-1, M8-2 and M8-3 gave a precursor ion at m/z 295.131 which was 16 Da larger than that of metabolite M4. Their elemental composition was $C_{15}H_{14}N_6O$, suggesting an

DMD #32326

oxidation metabolite of M4 (m/z 279.136, $C_{15}H_{14}N_6$). For M8-1, a fragment ion at m/z 278.118 resulted from a neutral loss of NH_3 , while m/z 105.053 was the same as that of M4, indicating that the pyridine group was intact, but the oxidation position could not be confirmed. M8-2 showed fragment ions at m/z 277.121, 263.106 and 262.108 which were identical to the parent drug, indicating that part A and the methyl group were intact. Hence, we concluded that the primary amine substituent group in M4 was hydroxylated. For M8-3, a fragment ions at m/z 277.121 resulted from a neutral loss of H_2O , supposing the formation of hydroxyl group. The major fragment ions of m/z 250.110, 173.084 and 156.056 showed that the pyridine-pyrimidine-amino group was intact. M8-3 was tentatively identified as a hydroxylation metabolite at methylpyridine moiety (See Fig. 6). Metabolite M9 gave a precursor ion at m/z 311.126 which was 32 Da larger than that of M4. Its elemental composition was $C_{15}H_{14}N_6O_2$, suggesting a dioxide of M4, but the structure could not be confirmed by the mass spectrum.

Metabolite M10. Metabolite M10, found in plasma and urine, eluted at 8.1 min with a precursor ion at m/z 321.148, which was 42 Da larger than that of M4. Its elemental composition was $C_{17}H_{16}N_6O$. The mass spectrum of M10 showed a major fragment ion at m/z 262.109, suggesting the modification occurred on the primary amine group. Metabolite M10 was identified as the acetylation metabolite of M4 on the primary amine substituent. The standard substance was synthesized chemically using acetic anhydride under room temperature. The chromatographic retention time and mass spectra of the standard substance were the same as that of M10. 1H and ^{13}C NMR data were obtained to confirm the structure. The standard compound was characterized as: 1H NMR (400 MHz, MeOD) δ : 9.30 (s, 1H), 8.69 (d, $J = 2.0$ Hz, 1H), 8.66 (d, $J = 6.0$ Hz, 1H), 8.59 (d, $J = 8.0$ Hz, 1H), 8.54 (d, $J = 5.2$ Hz, 1H), 8.40 (d, $J = 2.0$ Hz, 1H), 7.59 (dd, $J = 8.0, 4.8$ Hz, 1H), 7.45 (d, $J = 5.2$ Hz, 1H), 2.53 (s, 3H), 2.18 (s, 3H). ^{13}C NMR (400 MHz, MeOD) δ : 170.6, 162.3, 160.8, 159.2, 150.5, 147.6, 146.1, 135.4, 134.6, 134.5, 134.2, 133.0, 124.0, 122.6, 108.3, 22.3, 18.7. The

DMD #32326

NMR data of M10 are shown in Supplemental Data Fig. S11-S12.

Metabolite M11. Metabolite M11, found in urine, eluted at 8.2 min and gave a precursor ion at m/z 479.163 with a larger mass of 176 Da than that of M3. Its elemental composition was $C_{20}H_{25}F_3N_2O_8$, indicating a glucuronide conjugate of M3. The primary mass spectral fragment ions of M11 were m/z 303.131 and 203.030, which could be the glucuronide conjugate of M3. A chromatographic peak with the same retention time as that of M11 was detected in the extracted ion chromatogram of m/z 303.132 due to the in-source dissociation of M11 (Fig. 8A).

Metabolite M12. Metabolite M12, found in urine and feces, eluted at 22.7 min with a precursor ion at m/z 563.214. Its elemental composition was $C_{28}H_{25}F_3N_8O_2$, indicating the demethylation, dehydrogenation and oxidation of M0. In the mass spectrum, M12 showed one primary fragment ion at m/z 463.155, suggesting the methyl piperazine group was metabolized. M12 was identified as a carbonylation metabolite of M1 with lactam formation, but the exact position could not be confirmed by the mass spectrum.

Metabolite M13. Metabolite M13, found in urine and feces, eluted at 16.0 min with a precursor ion at m/z 565.225. The elemental composition of M13 was $C_{28}H_{27}F_3N_8O_2$, indicating the demethylation and oxidation of M0. The fragment ion at m/z 547.226 was generated by a neutral loss of H_2O . The primary mass spectral fragment ion of M13 was m/z 173.055, indicating that pyridine-pyrimidine-amino group was intact. M13 was tentatively identified as the hydroxylation metabolite of M1, but the exact position could not be confirmed.

Metabolite M14. Metabolite M14, found in plasma and urine, eluted at 20.2 min with a protonated precursor ion at m/z 577.229. Its elemental composition was $C_{29}H_{27}F_3N_8O_2$, indicating the introduction of an oxygen atom with dehydrogenation. The major fragment ion at m/z 463.150 showed that the modification occurred on the methyl piperazidine group. M14 was tentatively identified as a metabolite

DMD #32326

whith a lactam formation on the piperazine ring.

Metabolite M15. Metabolite 15-1, found in urine, eluted at 18.1 min, showing a protonated precursor ion at m/z 595.239, which was 32 Da larger than that of M0. The elemental composition of M15-1 was $C_{29}H_{29}F_3N_8O_3$, indicating a dioxide of M0. The major fragment ions at m/z 492.170 and 463.150 suggested the oxidation was located on the methyl piperazine group. A fragment ion at m/z 577.232 with a high relative abundance was produced by a neutral loss of H_2O , which indicated that a hydroxyl group was formed. M15-1 was identified as a dioxide of M0 on the methyl piperazine group. Metabolite M15-2 was eluted at 17.5 min in feces extracts, showing a protonated precursor ion at m/z 595.242, and its elemental composition was identical with M15-1. No obvious fragment ion was produced, and the oxidation site of M15-2 could not be confirmed.

Metabolite M16. Metabolites M16-1 and M16-2 were eluted at 11.8 and 18.5 min, respectively. Both showed a precursor ion at m/z 739.283, which was 176 Da larger than that of M0. Their mass spectra were identical and the major fragment ion was at m/z 563.246, indicating that two glucuronide conjugates of the parent drug M0 were produced, but the conjugation sites could not be confirmed. Two chromatographic peaks with the same retention time as that of M16-1 and M16-2 could be detected in the extracted ion chromatogram of m/z 563.248 due to the in-source dissociation of M16-1 and M16-2 (See Fig. 8B).

Metabolite M17. Metabolite M17, found in urine, eluted at 11.7 min with a precursor ion at m/z 725.267. M17 showed a major fragment ion at m/z 549.241, indicating a neutral loss of 176 Da. It was supposed that M17 was a glucuronide conjugate of M1. Similarly, a chromatographic peak with the same retention time as M17 could be found in the extracted ion chromatogram of m/z 549.234 due to the in-source dissociation of M17 (See Fig. 8C).

Metabolite M18. Metabolites M18-1, M18-2 and M18-3 showed a precursor ion at m/z 755.280 with a

DMD #32326

mass of 176 Da larger than m/z 579.244, indicating three glucuronide conjugates of flumatinib mono-oxide (M2). The mass spectra of M18-1 and M18-3 showed major fragment ions at m/z 479.145 and 279.096, 16 Da larger than m/z 463.148 and 263.105 of M0, respectively, suggesting that the oxidation site was on part A. The mass spectrum of M18-2 was similar to M2-1 and M2-6, indicating that part A was oxidized into an *N*-oxide. Three chromatographic peaks with the same retention time as those of M18-1, M18-2 and M18-3 could be detected in the extracted ion chromatogram of m/z 579.244 due to the in-source dissociation (data not shown).

Metabolite M19. Metabolite M19, found in urine, eluted at 12.8 min and showed a precursor ion at m/z 741.269. Its elemental composition was $C_{34}H_{35}F_3N_8O_8$. The major fragment ion at m/z 565.228 indicated a neutral loss of 176 Da, suggesting that M19 was a glucuronide conjugate of $C_{28}H_{27}F_3N_8O_2$. The minor fragment ions at m/z 479.146 and 279.100 showed that the corresponding phase I metabolite was a demethylation and oxidation product, and that the oxidation position was on part A.

Metabolite M20. Metabolite M20, found in feces, eluted at 19.5 min with a fragment ion at m/z 591.244 that had a 42 Da larger mass than M1. Its elemental composition was $C_{30}H_{29}F_3N_8O_2$, suggesting an acetylation metabolite of M1. The mass spectrum of M20 showed a major fragment ion at m/z 549.235 which was the same as the protonated molecular weight of M1. The minor fragment ions at m/z 463.151 showed that the piperazine group was the acetylation site. Comparison with the synthesized reference standard confirmed M20 to be an acetylation metabolite of M1. A chromatographic peak with the same retention time as that of M20 could be detected in the extracted ion chromatogram of m/z 549.234 due to the in-source dissociation of M20 (See Fig. 8D).

Discussion

The metabolism of flumatinib, a new tyrosine kinase inhibitor for treatment of chronic myelogenous leukemia (CML), was studied by UPLC/Q-TOF MS analysis of plasma, urine and feces of CML patients after oral administration during phase I trials. The chemical structures of the metabolites were characterized by their accurate mass, mass spectral fragmentation patterns, and comparison with the chemically synthesized reference standards.

After oral administration, flumatinib was extensively metabolized. Up to 13 metabolites were detected in plasma extracts. The most abundant drug related component in plasma extract was the parent drug. In addition to the unmetabolized flumatinib, the primary metabolites in plasma were *N*-desmethyl flumatinib (M1), a metabolite with similar pharmacological properties to flumatinib, and the amide hydrolysis product M3. The content of M3 in plasma was about 30% of that of the parent drug, based on the peak area percentage. Some minor metabolites in plasma included oxidation metabolites (M2-1, M2-4, M2-7, M2-9 and M14) and a hydrolysis metabolite (M4), which were further metabolized to form multiple metabolic products (M5, M6, M8-3, and M10). Furthermore, one glucuronide conjugate of parent drug M16-2 was detected in plasma.

In addition to the parent drug, a total of 30 metabolites were detected in urine. The primary metabolite in urine was the amide hydrolysis product M3, whose content was 3 times higher than that of unmetabolized parent drug. Other major metabolites included *N*-desmethyl flumatinib (M1), hydrolysis metabolite (M4), oxidation metabolites (M2-1 and M2-9) among others, which could be further metabolized into multiple metabolic products. Several phase II metabolites were also detected including the glucuronide conjugates of M0, M1, M2 and M3, and the acetylation product of M4.

After oral administration, a large amount unmetabolized parent drug was detected in feces, which could

DMD #32326

be explained either by the excretion through bile or by poor oral absorption of flumatinib. In addition to the parent drug, *N*-desmethyl metabolite (M1), *N*-demethylation coupled with oxidation metabolites (M12 and M13), oxidation metabolites of M0 (M2-1-M2-9, and M15-2), and one acetylation metabolite of M1 (M20) were excreted.

The major drug related components in circulation were the parent compound, *N*-desmethyl flumatinib (M1) and the amide hydrolytic metabolite (M3). M3 was the primary metabolite in both plasma and urine. Many metabolites related to hydrolysis metabolite M4 were detected in plasma and urine (i.e., M4, M8, M9 and M10), which suggested that the predominant metabolic pathway of flumatinib in human was amide hydrolysis. The relatively low amounts of M4 and its metabolites, compared to the parallel hydrolytic product M3 and its metabolites, was proposed that some of the metabolites related to M4 were probably missed out. The relationship of structure and metabolic pathways was analyzed and we concluded that there were at least two possible causes leading to the amide hydrolysis. First, the introduction of the trifluoromethyl electron-withdrawing group enhances the electrophilicity of the amide carbon atom that may facilitate hydrolysis of the amide bond. Second, the change from a phenyl ring in imatinib to a pyridine ring in flumatinib adds another electron-withdrawing group (Gschwind et al., 2005; Marull et al., 2006), and electron-withdrawal would be enhanced by protonation of the pyridine moiety. Such protonation may also provide a site for either an ionic bridge or hydrogen bond with esterase/amidase active site, and thereby increase the affinity of flumatinib for the enzyme. Stability tests of flumatinib in phosphate buffer (pH 7.4) incubated at 37°C for 2 hours and in plasma kept at room temperature for 2 hours proved that flumatinib was stable and that no *in vitro* degradation occurred. We therefore concluded that the amide hydrolytic reaction occurred only *in vivo*.

During the progress of this phase I clinical trial, the long-term toxicity tests of Sprague Dawley rat,

DMD #32326

beagle dog and cynomolgus monkey were assessed and plasma samples for toxicokinetics studies were collected. The remaining samples were used for metabolite identification using the identical UPLC/Q-TOF MS method used for human samples. In the study, there were large amounts of the parent drug, M0, in the plasma of rat, dog, monkey and human. The primary metabolites in circulation were similar in these four species and metabolite M3 was the most abundant metabolite especially in rat and dog with the peak areas more than 2 and 4 times that of M0, respectively. In addition, metabolites M4, M5 and M10 were other metabolites in rat plasma which peak areas were larger than 10% that of M0, M2-1 and M4 were the other primary metabolites in dog. No other primary metabolites were found in monkey and human (Table 2). These findings showed that after oral administration of flumatinib, the predominant metabolites were the products of amide hydrolysis (M3 and M4), and the metabolic profiles in plasma between these four species were qualitatively similar. Comparison with plasma from rats, dogs, and monkeys revealed no obviously exclusive metabolite in human plasma and the levels of major metabolites in human plasma were not disproportionately higher than in any of the animal species used during nonclinical toxicology testing. The results of the present study could probably provide some instructional information for clinical safety assessment of drug metabolites, even though no specific guidance for the safety assessment of drug metabolites for cancer therapies has yet been developed.

In summary, this study presented a metabolite characterization of flumatinib in humans. Flumatinib was extensively metabolized after oral administration, and the major metabolic pathways observed were amide hydrolysis, demethylation, oxidation, and glucuronide conjugation. In addition, the metabolic profiles for circulating flumatinib in test species were similar to those observed for humans, suggesting that the safety evaluation using these species in a nonclinical setting was suitable.

DMD #32326

Acknowledgments

We would like to thank Dr. Yuya Wang and Dr. Fanglong Yang for assistance with the synthesis and purification of reference standards. We also thank Dr. Tao Yuan for the support in NMR analysis.

References

- Bateman KP, Castro-Perez J, Wrona M, Shockcor JP, Yu K, Oballa R and Nicoll-Griffith DA (2007) MS^E with mass defect filtering for in vitro and in vivo metabolite identification. *Rapid Commun Mass Spectrom* **21**: 1485–1496.
- Deininger MW, Goldman JM and Melo JV (2000) The molecular biology of chronic myeloid leukemia. *Blood* **96**: 3343–3356.
- Gschwind HP, Pfaar U, Waldmeier F, Zollinger M, Sayer C, Zbinden P, Hayes M, Pokorny R, Seiberling M, Ben-Am M, Peng B and Gross G (2005) Metabolism and disposition of imatinib mesylate in healthy volunteers. *Drug Metab Dispos* **33**: 1503–1512.
- Kantarjian H, Giles F, Wunderle L, Bhalla K, O'Brien S, Wassmann B, Tanaka C, Manley P, Rae P, Mietlowski W, Bochinski K, Hochhaus A, Griffin JD, Hoelzer D, Albitar M, Dugan M, Cortes J, Alland L and Ottmann OG (2006) Nilotinib in imatinib-resistant CML and Philadelphia chromosome–positive ALL. *N Engl J Med* **354**: 2542-2551.
- Kulanthaivel P, Barbuch RJ, Davidson RS, Yi P, Renner GA, Mattiuz EL, Hadden CE, Goodwin LA and Ehlhardt WJ (2004) Selective reduction of N-oxides to amines: application to drug metabolism. *Drug Metab Dispos* **32**: 966–972.
- Marull M and Rochat B (2006) Fragmentation study of imatinib and characterization of new imatinib metabolites by liquid chromatography–triple-quadrupole and linear ion trap mass spectrometers. *J Mass Spectrom* **41**: 390-404.
- Ren R (2005) Mechanisms of BCR-ABL in the pathogenesis of chronic myelogenous leukaemia. *Nat Rev Cancer* **5**: 172-183.
- Sawyers CL (2001) Cancer treatment in the STI571 era: what will change? *J Clinl Oncol* **19**: 13s-16s.

DMD #32326

Seaton QF, Lawley CW and Akers HA (1984) The reduction of aliphatic and aromatic N-oxides to the corresponding amines with titanium (III) chloride. *Anal Biochem* **138**: 238-241.

Steinberg M (2007) Dasatinib: A tyrosine kinase inhibitor for the treatment of chronic myelogenous leukemia and Philadelphia chromosome-positive acute lymphoblastic leukemia. *Clin Ther* **29**: 2289-2308.

Sun PY, Lv AF, Yang BH, Hu CY and Wang WB (2008) Aminopyrimidine compounds and their salts, process for preparation and pharmaceutical use thereof. US20080312251.

Zhang HY, Zhu MS, Ray KL, Ma L and Zhang DL (2008) Mass defect profiles of biological matrices and the general applicability of mass defect filtering for metabolite detection. *Rapid Commun Mass Spectrom* **22**: 2082-2088.

DMD #32326

Footnote

This work was supported by the National Science & Technology Major Project “Key New Drug Creation and Manufacturing Program”, China (Number: 2009ZX09301-001).

Legends for figures

Fig. 1 Chemical structure of flumatinib (A) and imatinib (B). The molecular formula of flumatinib is $C_{29}H_{29}F_3N_8O$.

Fig. 2 Mass spectra of flumatinib (A) and imatinib (B) at high collision energy.

Fig. 3 Metabolic profiles of flumatinib after oral administration of 800 mg. (A) Pooled plasma samples collected at 3 h, 8 h and 12 h after an oral administration; (B) Pooled urine samples collected 0-12 h after an oral administration; (C) Feces samples collected after once daily administration for 28 days.

Fig. 4 Mass spectra of metabolite M2 ($M+H^+$ m/z 579.244) at high collision energy on Q-TOF mass spectrometer. (A) M2-1 and M2-6; (B) M2-4 and M2-7; (C) M2-8; (D) M2-9.

Fig. 5 MS^n ($n=1-5$) spectra of metabolite M3 standard ($M+H^+$ m/z 303) on a LCQ Advantage Ion Trap mass spectrometer under ESI positive mode and the proposed mass fragmentation pathways for M3.

Fig. 6 Mass spectra of metabolite M4 ($M+H^+$ m/z 279.136) and M8 ($M+H^+$ m/z 295.131) at high collision energy on Q-TOF mass spectrometer. (A) M4; (B) M8-1; (C) M8-2; (D) M8-3.

Fig. 7 Mass spectra of metabolite M6 ($M+H^+$ m/z 319.126) and M7 ($M+H^+$ m/z 317.113) at high collision energy on Q-TOF mass spectrometer. (A) M6; (B) M7.

DMD #32326

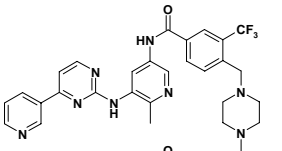
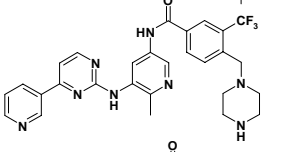
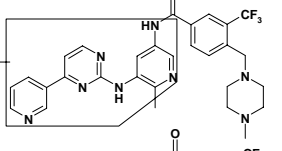
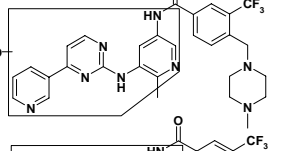
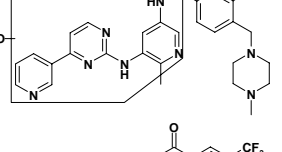
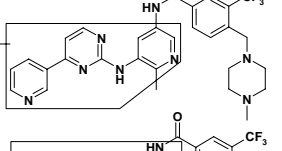
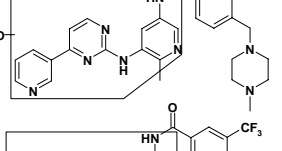
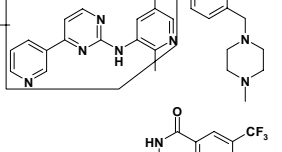
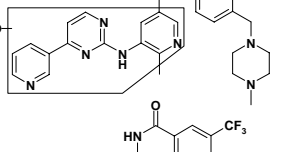
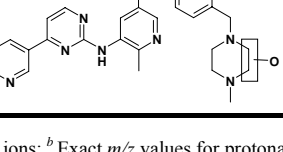
Fig. 8 Extracted ion chromatogram of flumatinib metabolites. The top panels in A, B, C and D represent phase I metabolite profiles, the bottom panels represent their corresponding phase II metabolite profiles. (* The chromatographic peak was formed because of in-source dissociation of their phase II metabolites)

Fig. 9 Identified metabolic processes of flumatinib in human. The major metabolic pathway was the amide hydrolysis. Details of chemical structures are shown in Table 1.

Tables

Table 1 Metabolite data for flumatinib in human plasma, urine and feces after oral administration

(P-plasma; U-urine; F-feces).

Metabolite	Proposed Formula	Proposed Chemical Structure	Retention Time (min)	M+H ⁺ ^a (M+H ⁺) ^b	Fragment Ions
Flumatinib M0	C ₂₉ H ₂₉ F ₃ N ₈ O		19.2 (P, U, F)	563.248 (563.250)	463.150, 449.132, 263.103, 262.102, 156.056
M1	C ₂₈ H ₂₇ F ₃ N ₈ O		19.1 (P, U, F)	549.234 (549.234)	463.149, 449.134, 263.105, 262.102
M2-1	C ₂₉ H ₂₉ F ₃ N ₈ O ₂		16.2 (P, U, F)	579.245 (579.244)	479.146, 463.148, 277.119, 263.105, 262.104
M2-2	C ₂₉ H ₂₉ F ₃ N ₈ O ₂		16.4 (F)	579.244 (579.244)	479.147, 279.093
M2-3	C ₂₉ H ₂₉ F ₃ N ₈ O ₂		17.0 (F)	579.246 (579.244)	479.142, 279.108
M2-4	C ₂₉ H ₂₉ F ₃ N ₈ O ₂		17.6 (P, U, F)	579.248 (579.244)	519.230, 479.146, 279.096, 278.101
M2-5	C ₂₉ H ₂₉ F ₃ N ₈ O ₂		18.4 (U, F)	579.247 (579.244)	479.143, 279.093
M2-6	C ₂₉ H ₂₉ F ₃ N ₈ O ₂		18.5 (U, F)	579.247 (579.244)	479.142, 463.147, 263.108, 262.108
M2-7	C ₂₉ H ₂₉ F ₃ N ₈ O ₂		19.6 (P, U, F)	579.245 (579.244)	479.147, 293.113, 279.101, 278.103
M2-8	C ₂₉ H ₂₉ F ₃ N ₈ O ₂		20.2 (U, F)	579.245 (579.244)	561.234, 462.140, 277.107

^a Measured *m/z* values for protonated ions; ^b Exact *m/z* values for protonated ions

Table 1—Continued.

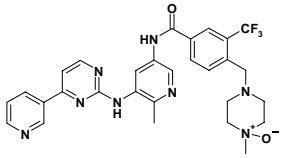
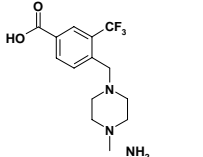
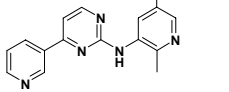
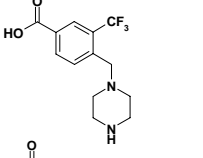
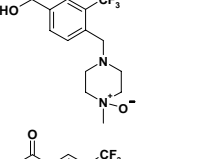
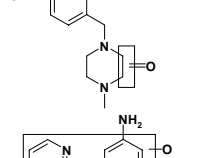
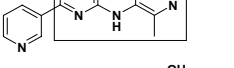
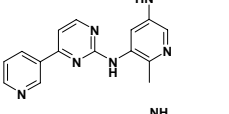
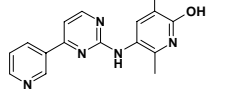
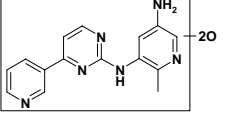
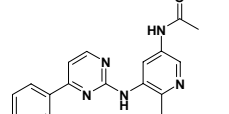
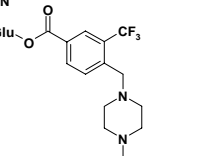
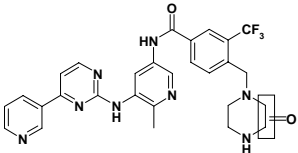
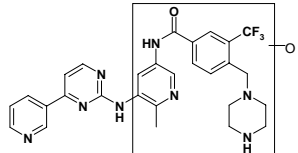
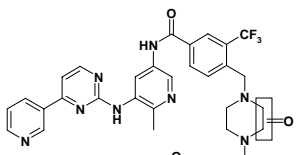
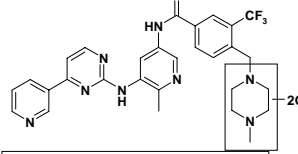
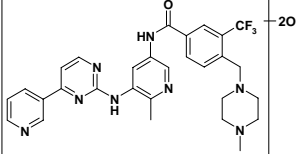
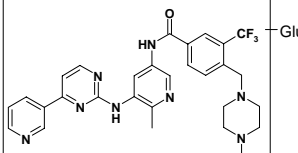
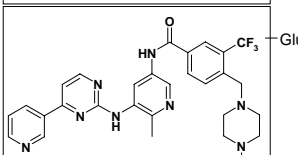
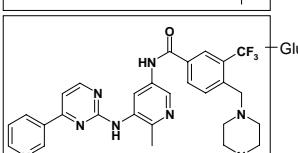
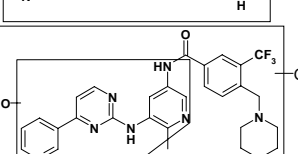
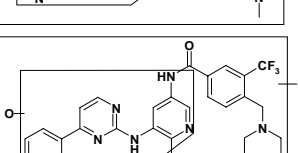
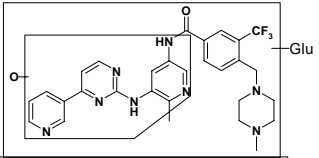
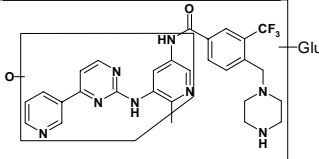
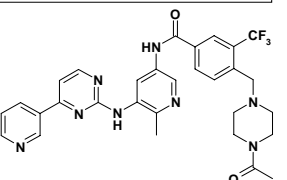
Metabolite	Proposed Formula	Proposed Chemical Structure	Retention Time (min)	M + H ⁺ ^a (M + H ⁺) ^b	Fragment Ions
M2-9	C ₂₉ H ₂₉ F ₃ N ₈ O ₂		21.3 (P, U, F)	579.244 (579.244)	492.178, 464.160, 263.104, 116.052
M3	C ₁₄ H ₁₇ F ₃ N ₂ O ₂		11.0 (P, U)	303.132 (303.132)	258.078, 203.032, 175.037, 100.100
M4	C ₁₅ H ₁₄ N ₆		5.8 (P, U)	279.136 (279.136)	262.111, 250.109, 235.099, 173.084, 156.058, 105.047, 78.035
M5	C ₁₃ H ₁₅ F ₃ N ₂ O ₂		10.5 (P, U)	289.112 (289.116)	203.033, 175.037, 85.078
M6	C ₁₄ H ₁₇ F ₃ N ₂ O ₃		15.2 (P, U)	319.126 (319.127)	301.115, 258.076, 203.030, 175.039
M7	C ₁₄ H ₁₅ F ₃ N ₂ O ₃		7.6 (U)	317.113 (317.111)	289.120, 271.058, 246.070, 203.037, 175.035
M8-1	C ₁₅ H ₁₄ N ₆ O		6.0 (U)	295.132 (295.131)	278.118, 105.053
M8-2	C ₁₅ H ₁₄ N ₆ O		6.7 (U)	295.131 (295.131)	277.121, 263.106, 262.108
M8-3	C ₁₅ H ₁₄ N ₆ O		7.0 (P, U)	295.131 (295.131)	278.113, 277.121, 250.110, 173.084, 156.056
M9	C ₁₅ H ₁₄ N ₆ O ₂		7.1 (U)	311.126 (311.126)	277.118, 266.105, 250.110
M10	C ₁₇ H ₁₆ N ₆ O		8.1 (P, U)	321.148 (321.146)	279.137, 262.109, 235.098
M11	C ₂₀ H ₂₅ F ₃ N ₂ O ₈		8.2 (U)	479.163 (479.164)	303.131, 203.030, 100.100, 58.066

Table 1—Continued.

Metabolite	Proposed Formula	Proposed Chemical Structure	Retention Time (min)	M + H ⁺ ^a (M + H ⁺) ^b	Fragment Ions
M12	C ₂₈ H ₂₅ F ₃ N ₈ O ₂		22.7 (U, F)	563.214 (563.213)	463.155
M13	C ₂₈ H ₂₇ F ₃ N ₈ O ₂		16.0 (U, F)	565.225 (565.229)	547.226, 173.055
M14	C ₂₉ H ₂₇ F ₃ N ₈ O ₂		20.2 (P, U)	577.229 (577.229)	549.271, 463.150, 277.138, 263.106
M15-1	C ₂₉ H ₂₉ F ₃ N ₈ O ₃		18.1 (U)	595.239 (595.239)	577.232, 492.170, 463.150, 263.105
M15-2	C ₂₉ H ₂₉ F ₃ N ₈ O ₃		17.5 (F)	595.242 (595.239)	
M16-1	C ₃₅ H ₃₇ F ₃ N ₈ O ₇		11.8 (U)	739.283 (739.282)	563.246, 464.157, 263.106
M16-2	C ₃₅ H ₃₇ F ₃ N ₈ O ₇		18.5 (P, U)	739.289 (739.282)	563.249, 464.157
M17	C ₃₄ H ₃₅ F ₃ N ₈ O ₇		11.7 (U)	725.267 (725.266)	549.241
M18-1	C ₃₅ H ₃₇ F ₃ N ₈ O ₈		13.3 (U)	755.280 (755.277)	579.246, 479.145, 279.096
M18-2	C ₃₅ H ₃₇ F ₃ N ₈ O ₈		15.9 (U)	755.267 (755.277)	561.241, 479.142, 463.147, 263.107, 262.101

DMD #32326

Table 1—Continued.

Metabolite	Proposed Formula	Proposed Chemical Structure	Retention Time (min)	M + H ⁺ ^a (M + H ⁺) ^b	Fragment Ions
M18-3	C ₃₅ H ₃₇ F ₃ N ₈ O ₈		17.3 (U)	755.270 (755.277)	579.244, 479.141, 279.094
M19	C ₃₄ H ₃₅ F ₃ N ₈ O ₈		12.8 (U)	741.269 (741.261)	565.228, 479.146, 279.100
M20	C ₃₀ H ₂₉ F ₃ N ₈ O ₂		19.5 (F)	591.244 (591.244)	549.235, 463.151, 263.105

DMD #32326

Table 2 Metabolite data of flumatinib in rat, dog, monkey and human plasma. Data represent the peak area ratios of the metabolite to the parent drug (%).

Metabolite	Rat	Dog	Monkey	Human
M0	100	100	100	100
M1	2.28	1.77	-	4.13
M2-1	1.40	11.9	-	5.65
M2-7	1.06	7.44	-	0.626
M2-9	1.79	6.05	-	7.16
M3	276	481	60.0	33.5
M4	79.6	63.4	2.68	1.20
M5	28.2	9.47	2.61	0.519
M8-2	2.50	-	-	-
M8-3	4.59	-	-	0.479
M8-4	3.29	4.33	-	-
M10	114	-	0.958	1.54
M16-2	-	-	-	2.63
M17	6.16	-	-	-
M0'	-	-	3.14	-

- Not detected.

Figure 1

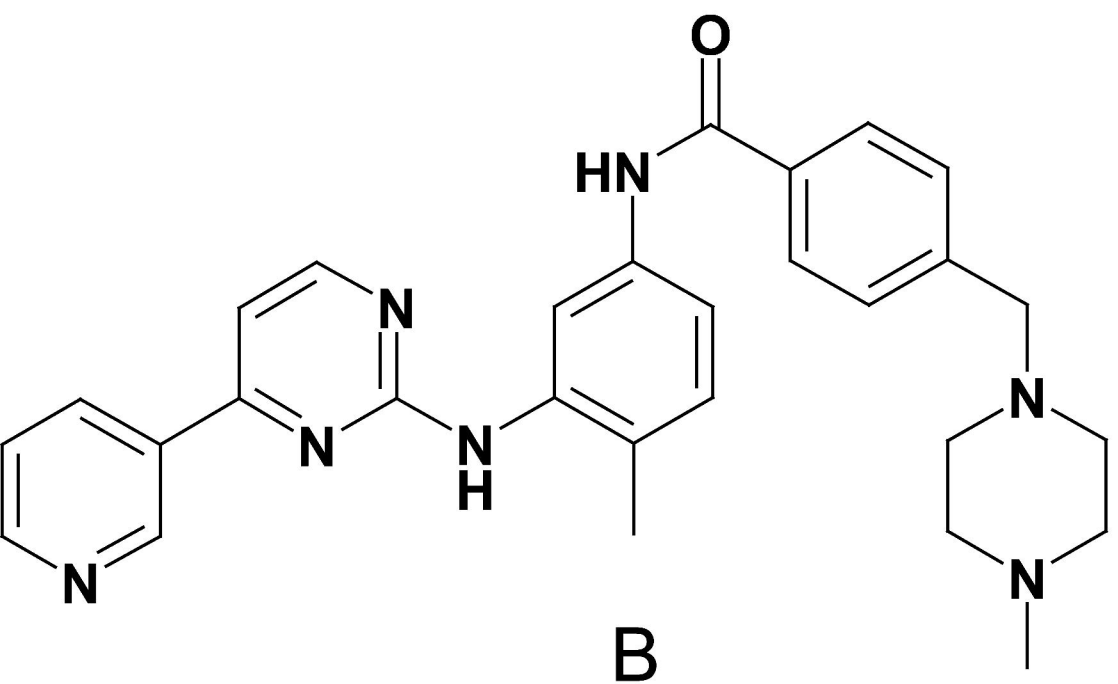
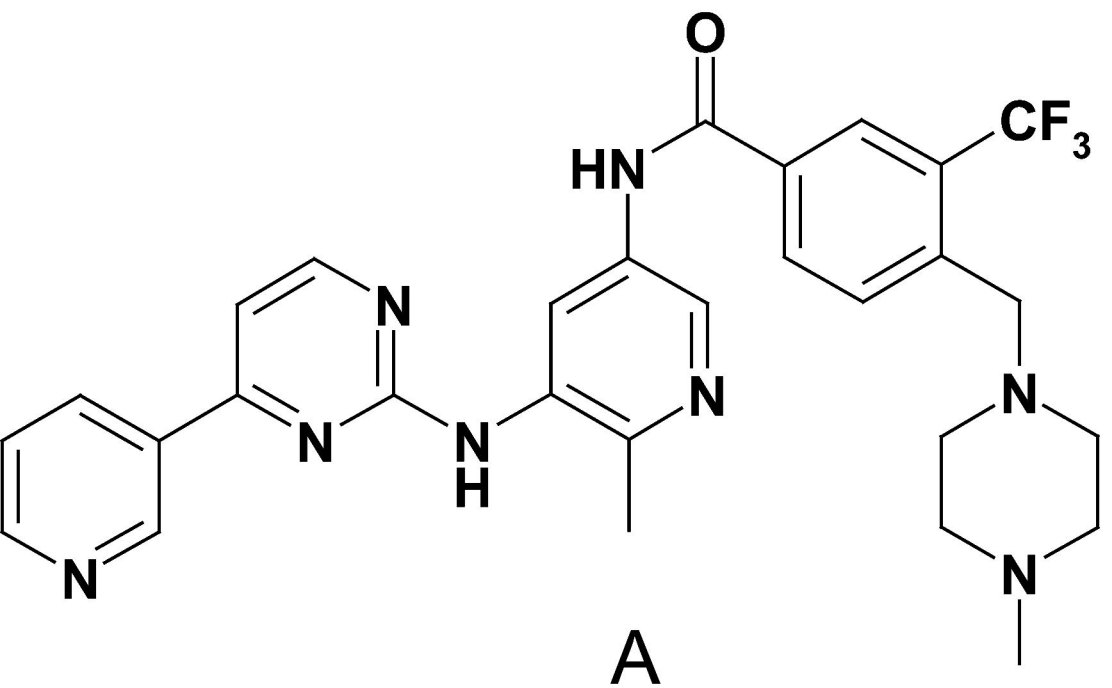


Figure 2

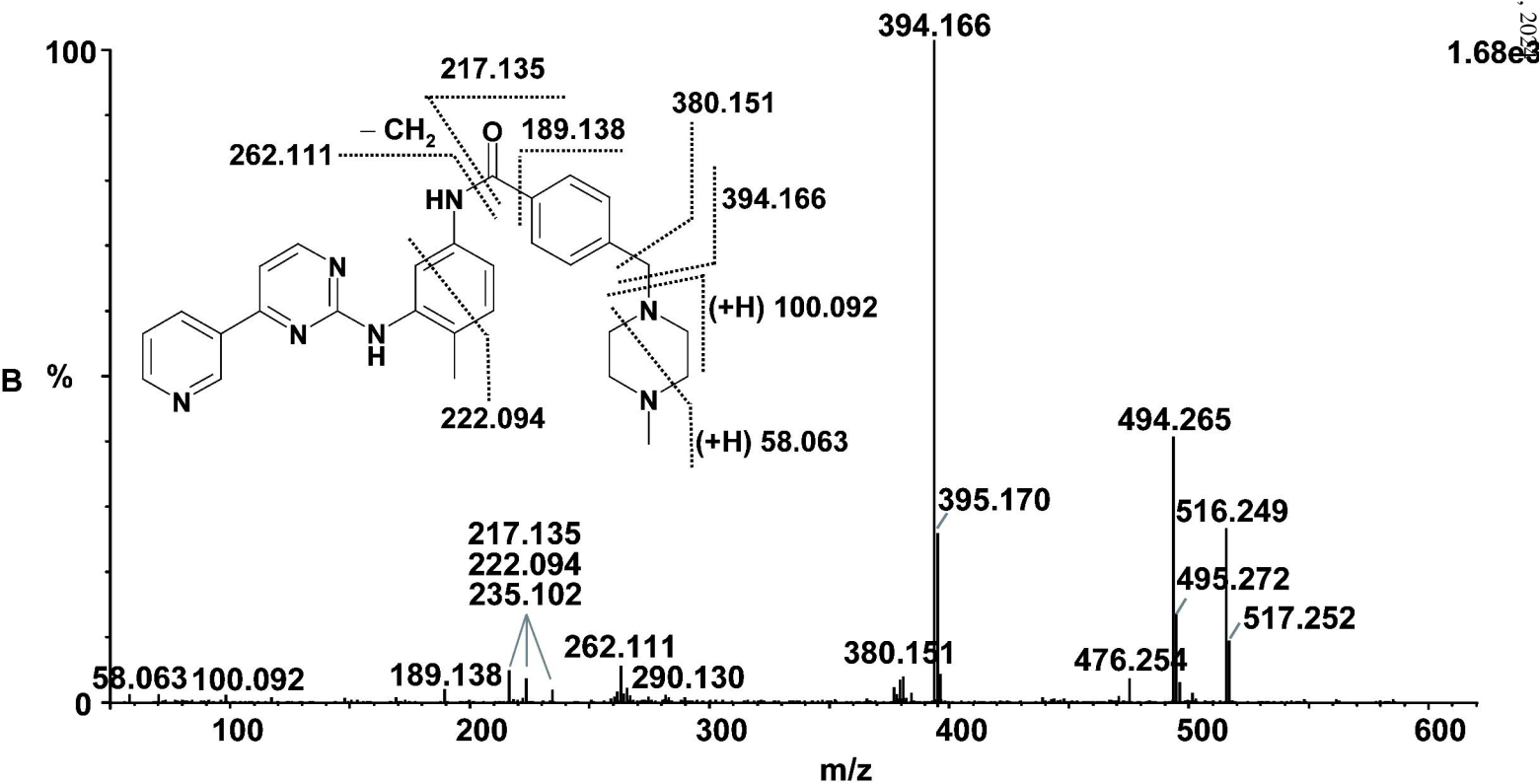
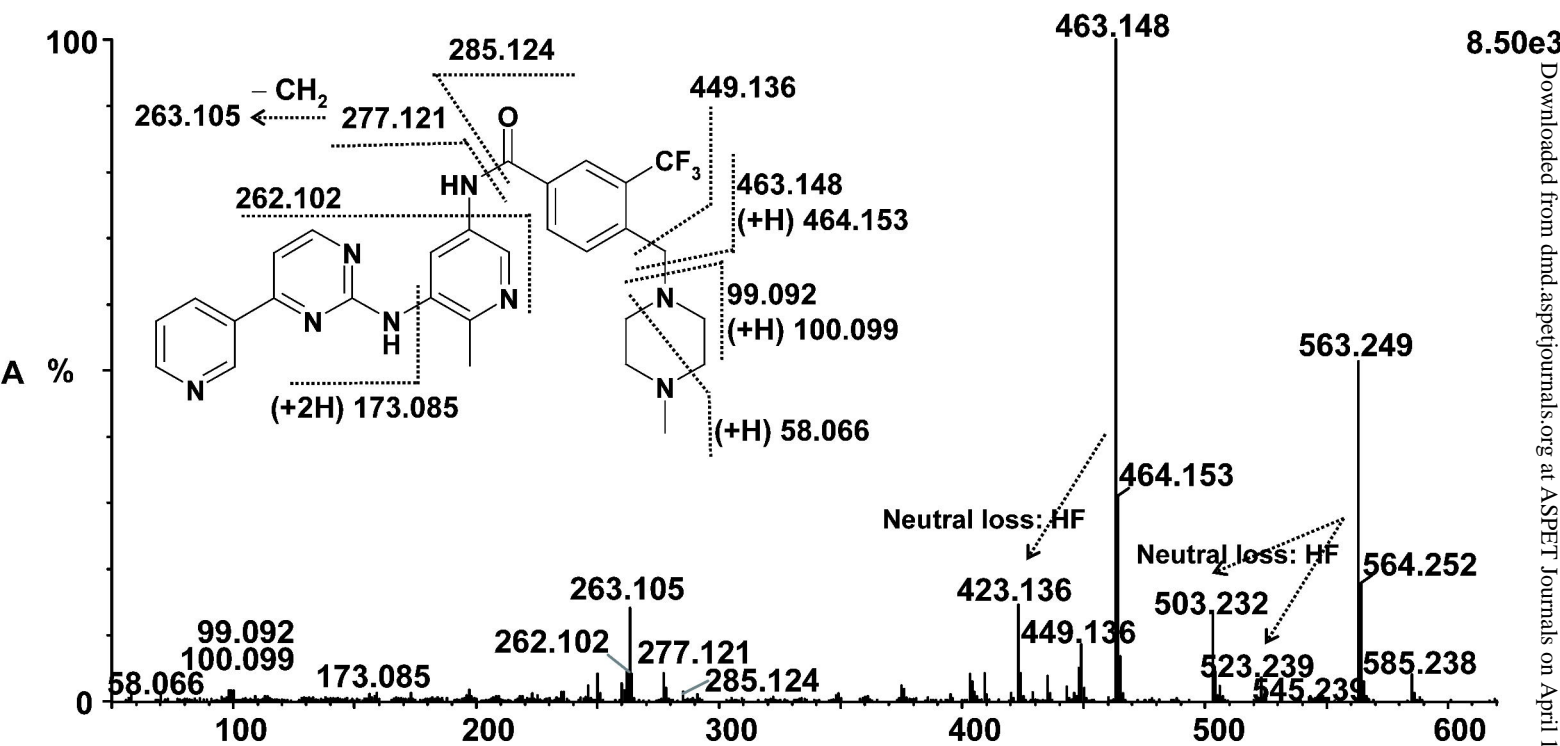


Figure 3

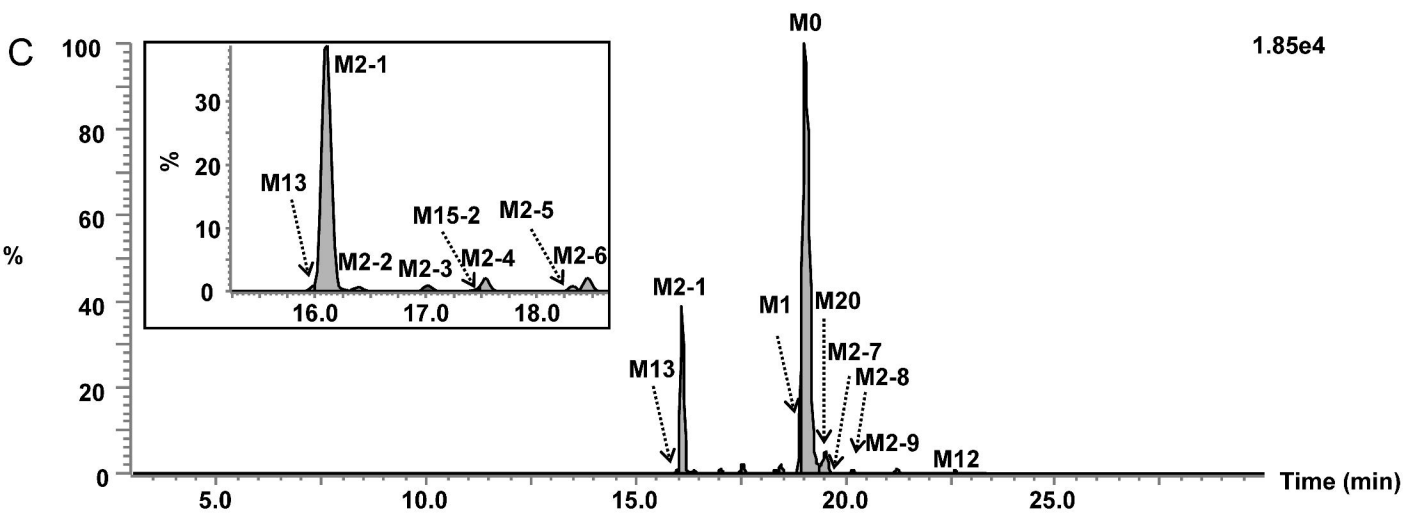
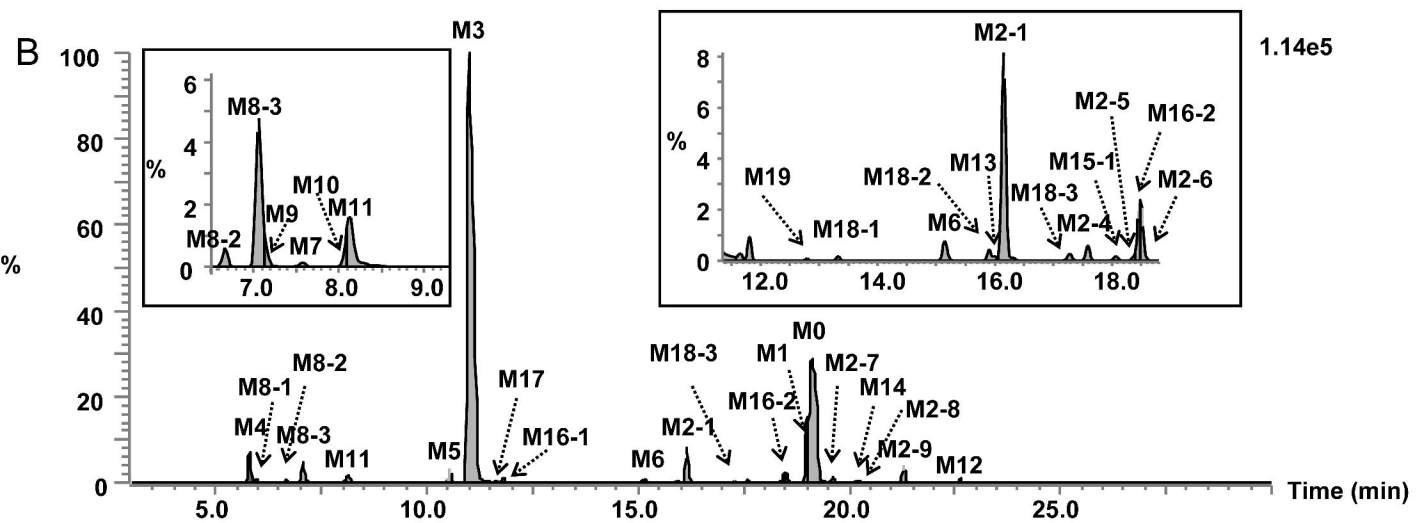
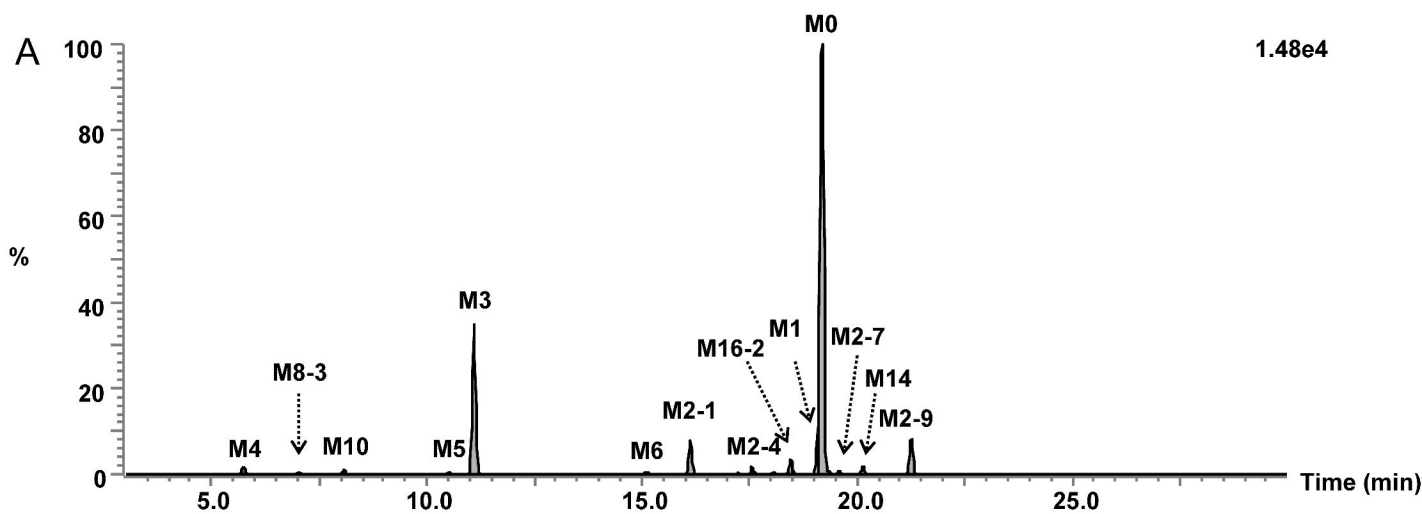


Figure 4

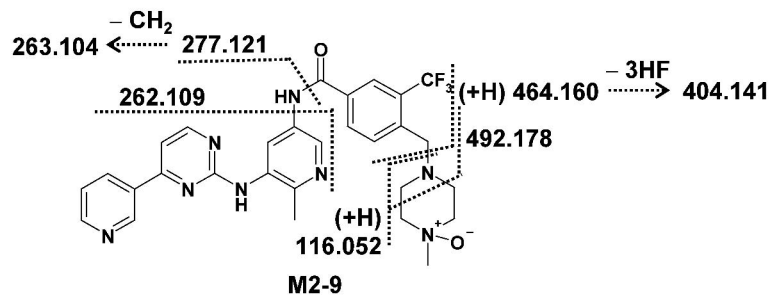
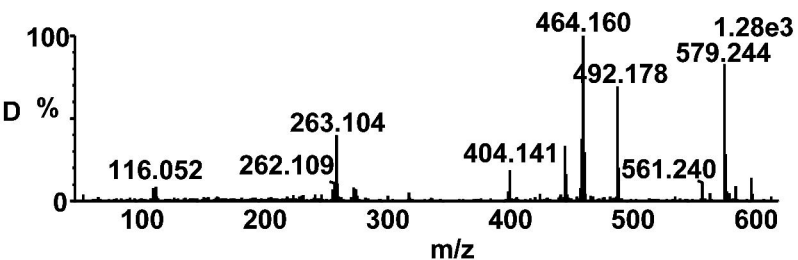
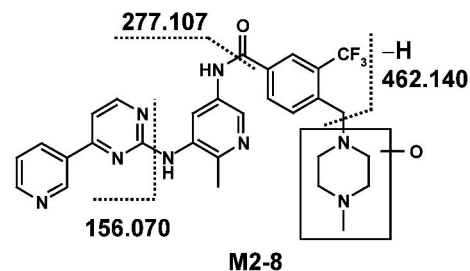
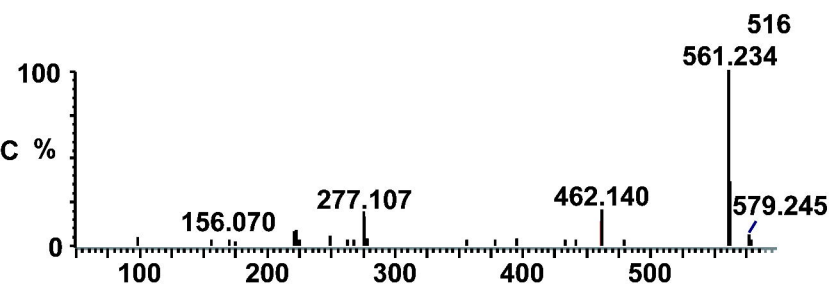
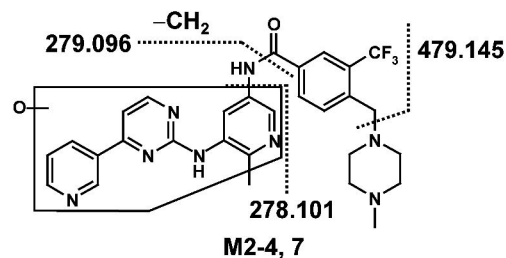
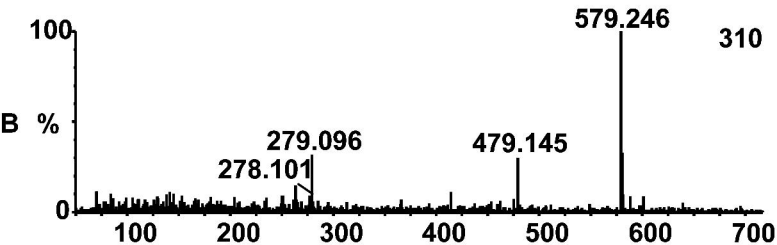
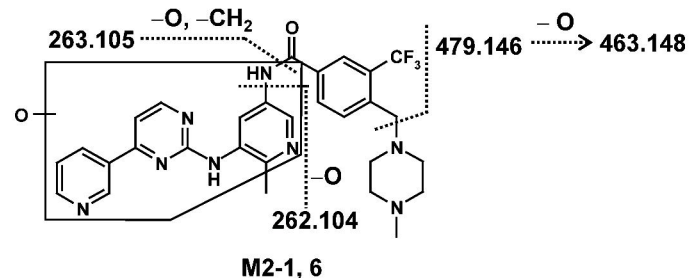
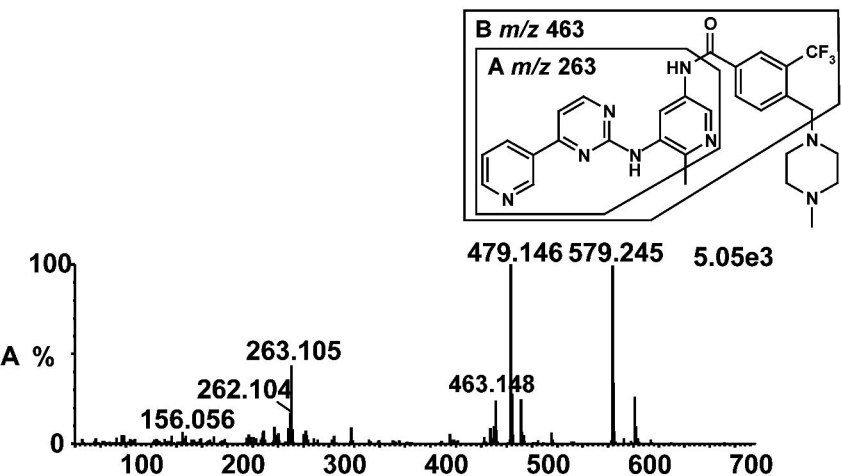


Figure 5

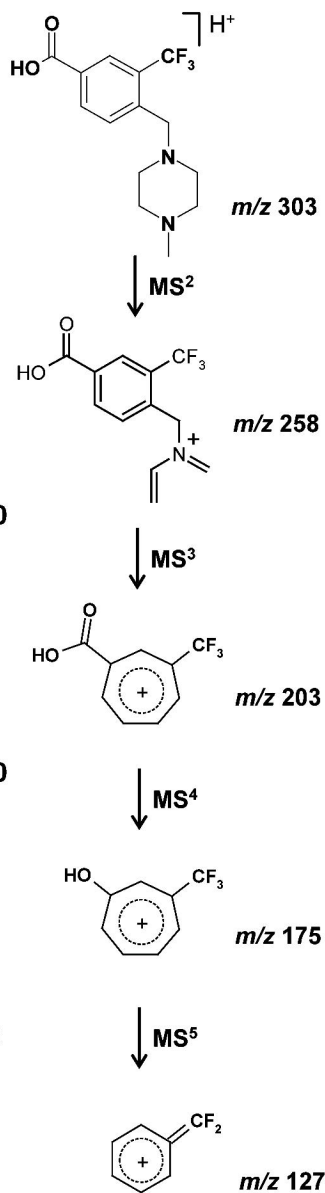
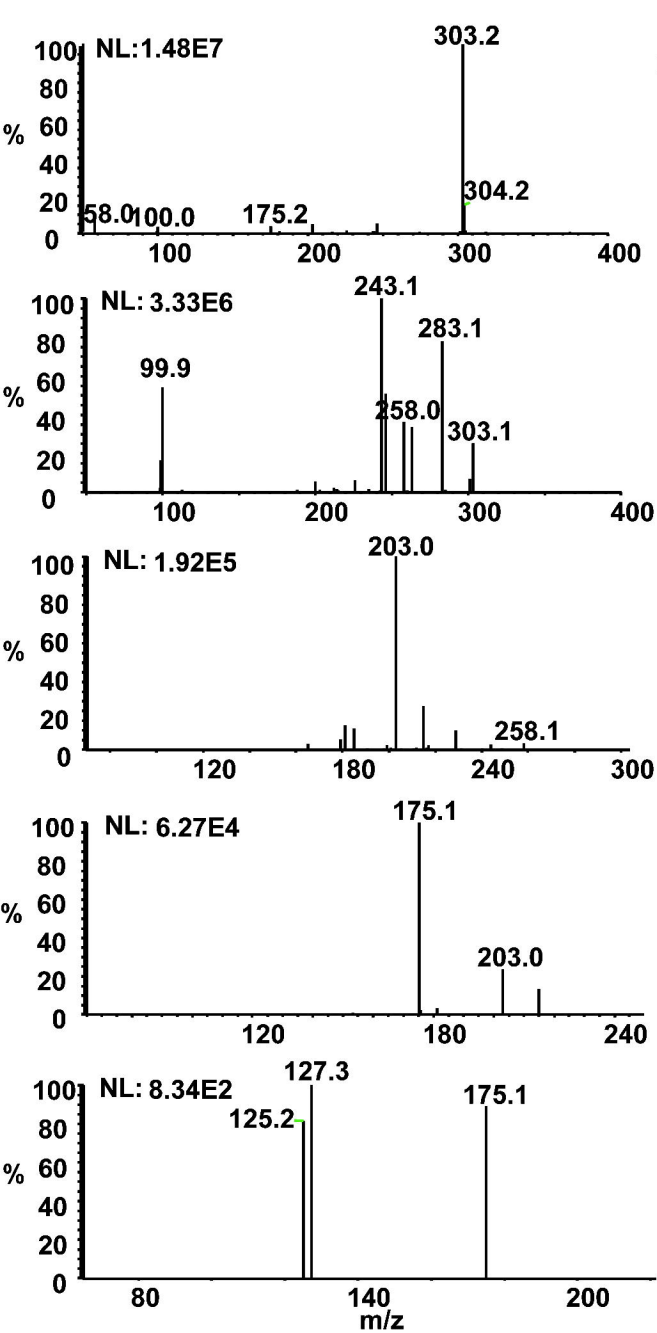


Figure 6

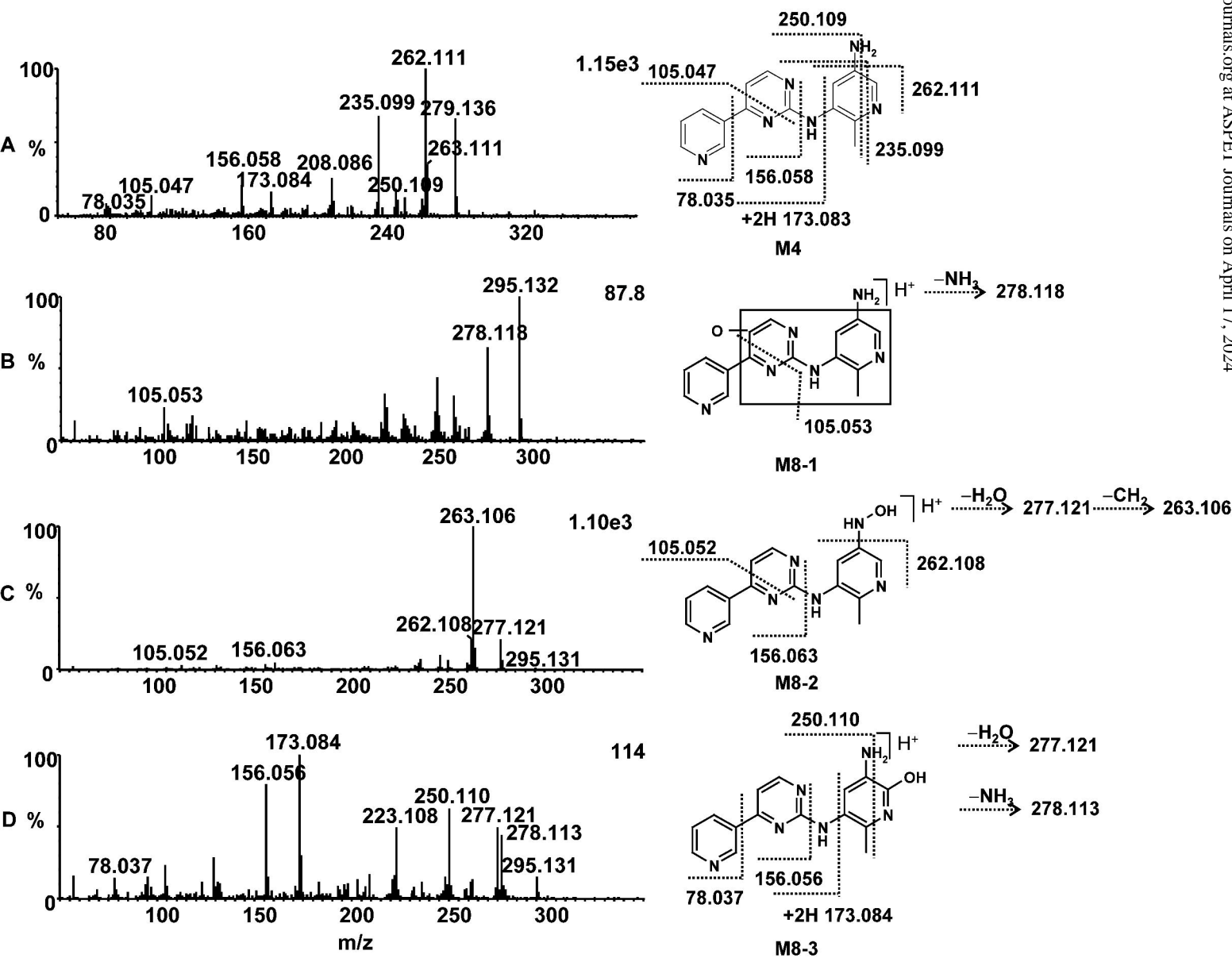


Figure 7

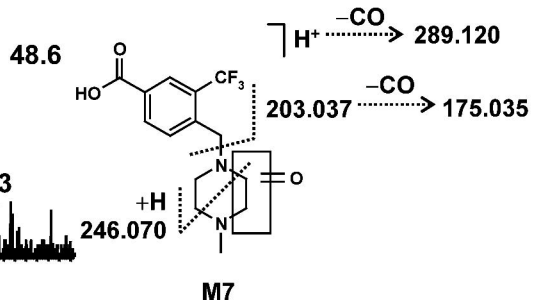
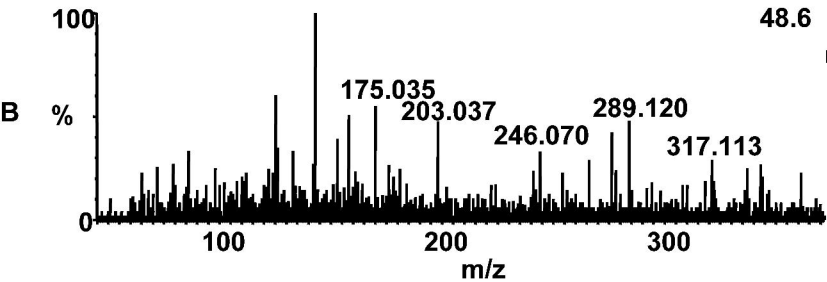
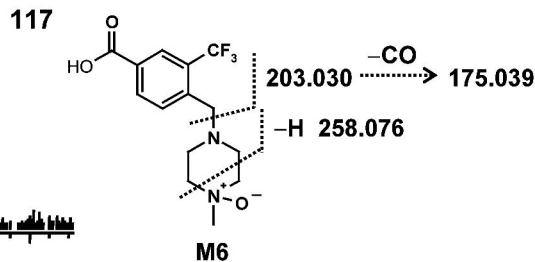
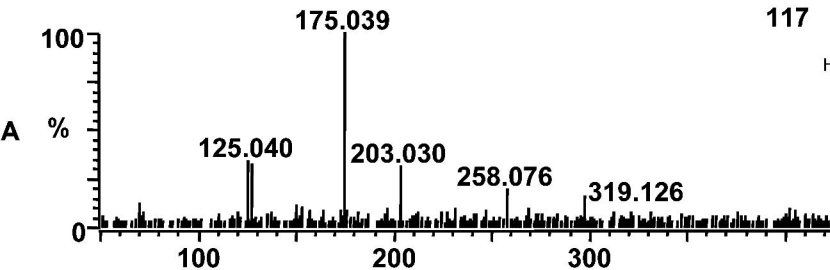


Figure 8

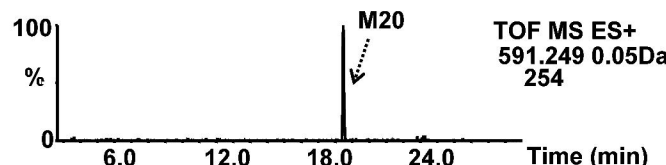
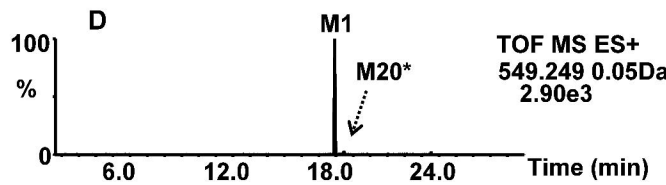
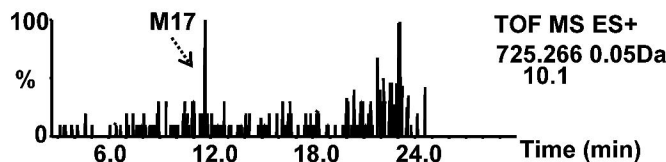
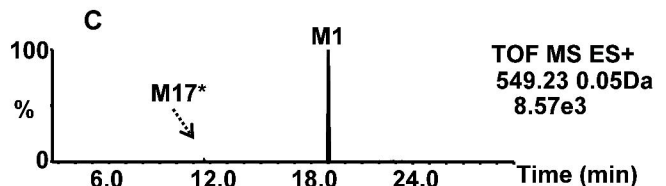
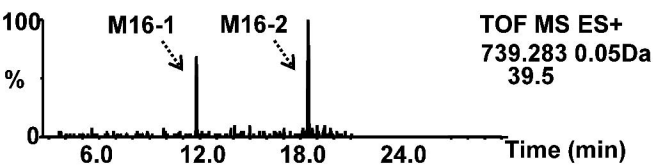
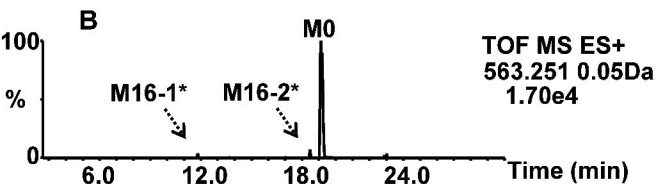
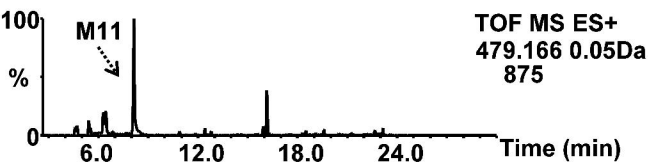
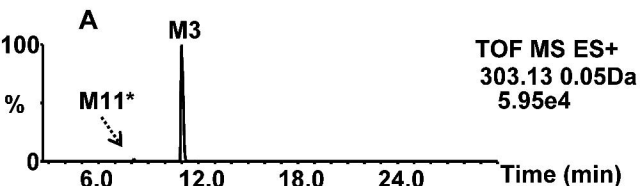


Figure 9

